https://doi.org/10.36375/prepare_u.iiche.a386

XRD analysis of nanosized silicon derived from broken glassware

Moulie Ghosh[a], Snigdha Khuntia[a], Sridhar Dalai[a*]
[a]*School of Engineering and Applied Science, Ahmedabad University, Ahmedabad, Gujarat 380009, India*
*Email: sridhar.dalai@ahduni.edu.in

Abstract

Recently silicon (Si) nanomaterial has drawn substantial interest owing to its versatility in chemical, and physical characteristics. The reduced size, and high surface area, unlike the bulk Si, has made it appropriate for diverse applications. There are numerous sources reported so far responsible for the production of nanostructured Si. However, the advantage of using broken glassware is that it doesn't require to undergo any purification process such as pre-heating or pre-acid leaching. Herein, we describe the synthesis of silicon nanomaterial from broken glassware collected from the laboratory employing the magnesiothermic reduction method. To explore the structure-property relationship, X-ray diffraction (XRD) patterns act as the fingerprint of the material. XRD study has been performed to qualitatively and quantitatively analyze the synthesized nanomaterial. From the qualitative analysis, the diffraction pattern observed after heat treatment has exhibited the formation of Si along with magnesium oxide (MgO) and magnesium silicate (Mg_2SiO_4). Whereas after the subsequent HCl and HF leaching, peaks for only Si have been observed. Incorporating Scherrer's Equation on the intense (111) plane, the crystallite size of Si has been estimated to be 49 nm. Using Rietveld analysis, the weight percentage of Si has been found to increase gradually with each treatment step.

Keywords: *Laboratory glass; Silicon; Nanomaterial; XRD; Rietveld analysis; Crystalline solid*

1. Introduction

The application of Silicon (Si) nanomaterial has made a tremendous impact on a broad range of fields including energy, sensors, catalysis, optoelectronics, photonics and biology (Chan et al. 2008; Betty 2008; perrone donnorso et al. 2012; Peng et al. 2013; Priolo et al. 2014; Wang and He 2017; Chandra Muduli and Kale 2023). It has been a widely used semiconducting material because of the attractive merits such as the rich abundance, and favourable biocompatibility (Kuang et al. 2015; Pakuła et al. 2023). Additionally it is worth pointing out the attractive features such as the controllable surface, excellent physical, chemical, mechanical, optical, electronic and catalytic properties, large surface to volume ratio which makes it a promising candidate for various application (Betty 2008; He et al. 2010; Falk et al. 2019). As a result, it has motivated to investigate and develop various nanostructures to meet the increasing demand of Si based applications. Several methods to produce crystalline Si nanostructures have been developed such as laser induced pyrolysis of Silane, chemical vapor deposition of Silane, metal assisted chemical etching of electronic grade crystalline silicon wafers, electrochemical anodization of crystalline wafers, oxidation of metal silicides, microemulsion technique and the convention carbothermal reduction (Kumar et al. 2012; Favors et al. 2015). However, many of these methods lack the scalabilty due to the involvement of expensive set up, intensive energy consumption and high cost and toxic precursor. Si can be found in many natural sources as it exists in oxide form as Silicon

dioxide (Si). Also, SiO_2 can be found in many industrial wastes as well. These nanostructures of Si can be prepared from wide range of inexpensive SiO_2 sources such as clay minerals, sand, coal, rice husk, bamboo leaves, sugarcane bagasse, and some indurtial sources like LCD, glass fibre, windshield (Favors et al. 2015; Ryu et al. 2016; Silviana and Bayu 2018; Furquan et al. 2018; Choi et al. 2018; Kang et al. 2019, 2020; Falk et al. 2019). Among many of the SiO_2 sources waste glassware could be an attractive source for Si production. Making effective use of discarded glassware can contribute in an excellent way to the solid waste management. The SiO_2 content in the glassware can be directly reduced to Si nanomaterial via magnesiothermic reduction method without undergoing any pre-treatment (Bao et al. 2007; Entwistle et al. 2018; Ghosh et al. 2022; Bristogianni and Oikonomopoulou 2022).

For understanding the sizes, shapes, and morphology of any nanomaterial various characterization techniques are required for the measurement. X- ray diffractometry (XRD) is one of the techniques adopted for the characterization of the nanomaterials and hence considered to be the fingerprint of the substance. It is a nondestructive and non- contact analytical technique. For accurate quantification of the interfacial atomic arrangements, the XRD intensities can be measured. The principle of XRD is based upon the Bragg's Law ($\lambda = 2d\sin\theta$) that relates the wavelength (λ) of the incident radiations to the distance between the two adjacent planes (d) and the diffraction angle (θ) (Rao and Biswas 2009; Sharma et al. 2012; Boddolla).

The present work aims to investigate the potential use of glass as an alternative source of SiO_2 and its reduction to Si using the XRD analysis. The XRD results have also been supported by the other characterization techniques such as Raman spectroscopy, Scanning Electron Microscopy, and Transmission Electron Microscopy.

2. Materials and methods

2.1 Materials

All the chemicals were used without further purification. Magnesium powder, Hydrochloric acid, and Hydrofluoric acid were purchased from Merck India Pvt. Ltd. The feed waste glassware was collected from the Laboratory and then crushed followed by grinding into fine powder.

2.2 Methods

2.2.1 Synthesis of Si Nanomaterial

Glass powder and Magnesium powder with 1:1 wt. ratio was homogeneously mixed using the mortar pestle and transferred to a crucible. The crucible filled with the mixture of glass powder and Mg powder was kept in the muffle furnace. The muffle furnace was heated with a heating ramp rate of 5 $^oCmin^{-1}$ and maintained at 650 ^oC for 5 h. After naturally cooling to room temperature, the heat-treated sample was collected and leached with 5 M of hydrochloric acid followed by subsequent washing with deionized water. Then the sample was dried in a hot air oven at 80 ^oC for 12 h. The obtained sample was then immersed in hydrofluoric acid (HF) for 1 h and repeatedly washed with deionized water. The product was finally dried at 80 ^oC for 12 h in a hot air oven. After drying the sample was collected and labelled GM_BH, GM_AH, GM_HCl, SiNM where G and M stand for Glass and Magnesium respectively, BH, AH, HCl stand for Before heat treatment, After heat treatment, HCl treated samples respectively and the final product has been denoted as SiNM which indicates the Silicon nanomaterial. These samples were further used for characterization.

2.2.2 Characterization of Material Properties

https://doi.org/10.36375/prepare_u.iiche.a386

The formation of the sample was confirmed by subjecting it different characterization techniques.

The crystal structure and phase evolution of the samples were investigated by powder X-ray diffractometry. The patterns were recorded on Rigaku Miniflex 600, using Cu K□ source having radiation of wavelength 1.54Å operated at 40 kV and 15 mA. This has been operated within an angular scan range (2□□ from 10º - 80º at a scanning speed of 2ºmin^{-1} and a step size set to 0.02º. The crystalline phases present in the samples were determined by comparing the peak positions and intensities with those listed in the Powder Diffraction File (PDF 2) data base. To further confirm the structural information and purity Raman spectroscopy was employed by using a Labram HR 10 Confocal Micro- Raman spectrometer at an excitation wavelength of 532 nm. The morphology of the prepared material was determined by JEOL JSM 7600 F Field Emission Gun-Scanning Electron Microscope (FEG-SEM) equipped with Energy Dispersive X-ray (EDX). The High-Resolution Transmission Electron Microscopy (HRTEM) Micrograph was obtained using Talos F200i S/TEM operated at 200 kV.

3. Results and discussions

The Si nanomaterial has been synthesized via magnesiothermic reduction of waste glassware collected from the laboratory in a muffle furnace. In order to clearly identify the phase transformation of amorphous glass to crystalline Si, the powder XRD analysis has been performed and shown in Fig. 1. The diffraction patterns of the feed glass (WG), reducing agent magnesium (Mg) along with the samples after every treatment steps (GM_AH, GM_HCl) and product (SiNM) have been compared in Fig. 1a. Every diffractogram has been measured in the angular range of 2θ between 10º - 80 º. The feed glass exhibited a noticeable broad hump near 22 º that corresponds to the amorphous phase of the SiO_2. The reducing agent Mg powder exhibited sharp crystalline peaks at 2Ɵ 32.1º, 34.3 º, 36.5 º, 47.7 º, 57.3 º, 63 º, 68.6 º, and 70 º that is attributed to the hexagonal crystal system of Mg phase (PDF card no. 01-071-4618). After heat treatment of the glass and Mg powder mixture, the reduced coarse sample (GM_AH) showed the sharp peaks of Si along with the phases of Magnesium oxide (MgO) and Magnesium silicate (Mg_2SiO_4). The XRD pattern of the reduced sample has been well matched with the PDF card of the Si (PDF card no. 00-005-0565), MgO (PDF card no. 01-076-2583) and Mg_2SiO_4 (PDF card no. 01-077-9267) shown in Fig. 1b and in Fig. 1c and 1d exhibits the attribution of Si, MgO phases to the cubic crystal structure whereas Fig. 1e reveals the orthorhombic crystal structure of Mg_2SiO_4. The missing of the broad hump near 22 º and the peaks corresponding to the Mg phase suggests the effective reduction of SiO_2 to Si and conversion of Mg to Mg- byproducts. Further on treatment with HCl acid, the sample (GM_HCl) shown the distinct five peaks of Si, which is attributed to the dissolving of MgO and Mg_2SiO_4 using HCl and removal of the Mg salts after subsequent washing with deionized water. The XRD analysis performed on the final product (SiNM) exhibited five obvious peaks which can be indexed to the cubic phase of Si. The XRD peaks obtained at 2θ of 28.8º, 47.8º, 56.7º, 69.7ºand 77.1º are correspond to the hkl (111), (220), (311), (400), and (331) respectively. The sharp peaks obtained are attributed to the formation of crystalline Si. However, it has been observed that the crystallinity has not been affected of the final product after etching with HF acid.

https://doi.org/10.36375/prepare_u.iiche.a386

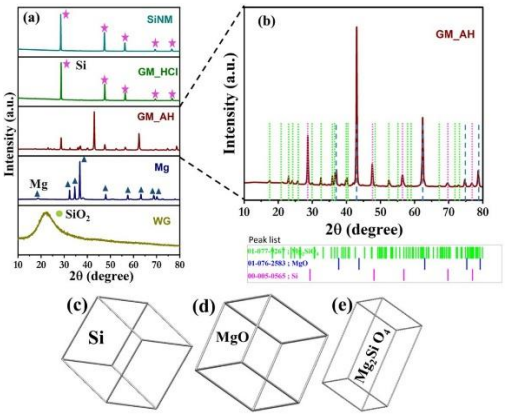

Fig. 1 XRD pattern (a) waste glass (WG, bottom), Mg powder (Mg), After heat treated sample (GM_AH), After HCl leached (GM_HCl), Final Product (SiNM); (b)magnified After heat treated sample (GM_AH) along with peak matching; Crystal Structure of phases (c)Si ; (d) MgO ; (e) Mg_2SiO_4

The XRD results has been corroborated with the phase quantification performed using the Rietveld method. Using the Rietveld analysis, the phase distribution has been measured and demonstrated in Fig. 2. It is clearly observed from the Fig. 2a, the Si content increased from 19.1% to 96.7 % in comparison with the other two phases (MgO and Mg_2SiO_4). It is also evident that the formation of Mg_2SiO_4 phase is almost negligible. However most of the MgO produced after heat treatment, eventually gets lowered after two step acid leaching. This again suggests the proper removal of the Mg byproduct after acid leaching and also the less favouring of the side reaction between MgO formed at the interface and the unreacted SiO_2 to form Mg_2SiO_4.

The diffraction pattern of SiNM has been further analyzed by Rietveld refinement program. The XRD profile correspond to the cubic phase structure along with the space group

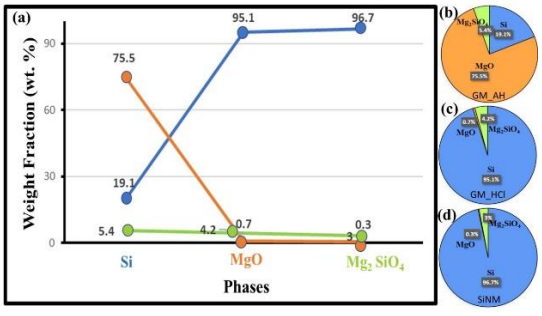

Fig. 2 (a) Quantitative phase analysis using Rietveld Method; Pie chart for the phase distribution (b) GM_AH, (c) GM_HCl, (d) SiNM

of Fd-3m. The Rietveld refinement parameter values obtained as profile R-factor (Rp): 4.21%, weighted profile R-factor (R_{wp}): 6.51%, expected R-factor (R_{exp}): 2.71%, and goodness of fit (χ^2): 7.39%. The fitted parameter values agree with the crystallographic model and the experimental XRD data. The primary crystallite size of SiNM has been found to be in the range of 45 nm - 50 nm, determined by the Debye Scherrer's Equation (Eq.1) and considering the FWHM correspond to the intense peak assigned to (111) plane.

$$\mathbf{D} = \frac{\mathbf{k\lambda}}{\mathbf{\beta cos\theta}} \qquad \text{Eq.1}$$

where D is the crystallite size, k is the shape factor, λ is the wavelength, β is the FWHM, 2Θ is the Bragg's angle.

The interplanar distance related to the (111) plane and the lattice parameter a for the cubic phase of Si has been estimated using the Bragg;s Equation (Eq.2) and found to be 3.137Å and 5.43 Å respectively.

$$\mathbf{n\lambda = 2dsin\theta} \qquad \text{Eq.2}$$

Furthermore, as a complement to XRD analysis, both the crystallinity and purity has been confirmed by the Raman analysis shown in Fig. 3 The Raman spectrum

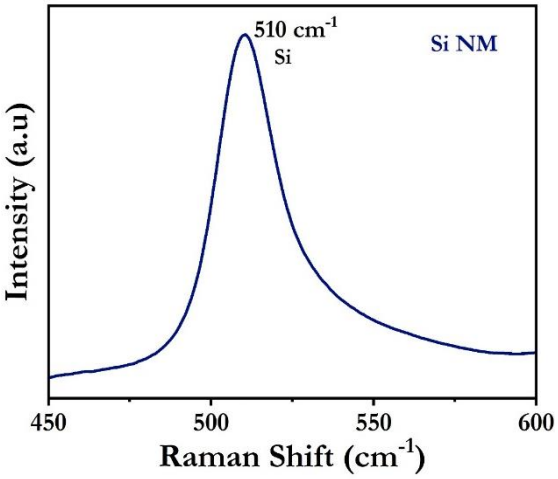

Fig. 3 Raman Spectroscopy of SiNM

of the final product (SiNM) after HF treatment depicted a clear peak at 510 cm^{-1}

that corresponds to the crystalline Si. Additionally, the absence of amorphous peak of Si at 480 cm^{-1} implies the crystalline phase of Si. The distinct peak at 510 cm^{-1} which is much lower than the bulk Si at 520 cm^{-1} suggests the formation of nano-scaled Si.

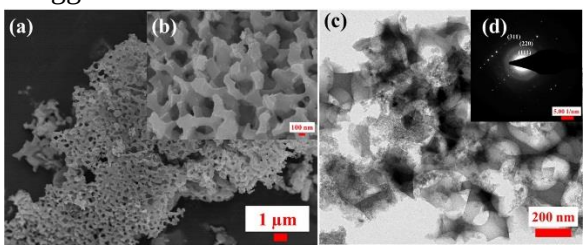

Fig. 4 SEM image of SiNM (a) low magnification, (b) high magnification (inset); (c) HRTEM image of SiNM, (d) SAED pattern of SiNM (inset)

The morphology of the product (SiNM) after magnesiothermic reduction and two step acid leaching process has been investigated by FESEM and HRTEM shown in Fig.4. The FESEM image in Fig 4a and 4b revealed the highly porous matrix of crystalline Si nanomaterial. The porosity can be attributed to the selective elimination of the imbedded Mg by-products such as MgO and Mg_2SiO_4 phases. The HRTEM image in Fig. 4c has also confirmed the formation of the porous network. The selected area electron diffraction pattern shown in Fig. 4d (inset) exhibited the (111), (220) and (311) is also in consistent with the XRD pattern of SiNM and moreover the dots observed in the pattern confirms the polycrystallinity of the material. The SiNM produced using the waste laboratory glassware found to be pure as determined by the XRD, Raman, SEM and TEM analysis.

4. Conclusion

In summary, Si nanomaterial was fabricated through magnesiothermic reduction using waste laboratory glassware as an alternative source of SiO_2. To confirm the formation of the material the present study was concerned to retrieve the important information related to the phase transformation, phase content, crystallographic structure, space group, lattice parameter, interplanar distance, crystallite size using the X-ray Diffractometry Analysis. The study revealed the conversion of amorphous SiO_2 contained in the waste glass feed to crystalline Si nanomaterial through the XRD patterns. The wt % of the cubic phase Si coupled with cubic phase of MgO and orthorhombic Mg_2SiO_4 phase have been observed where Si content found to be higher with negligible amount of Mg_2SiO_4 and reduced content of MgO. The average domain size of SiNM was found to range between 45- 50 nm. The Raman, FESEM and HRTEM analysis further complimented the XRD results and confirmed the formation of pure Si nanomaterial from waste laboratory glassware.

Acknowledgment

The authors express their gratitude to School of Engineering and Applied Science, Ahmedabad University for offering the laboratory and instrumental facilities. The authors would also like to acknowledge the financial support received by Ahmedabad University under seed grant through Grant no. URBSEASI22A1/SG/22-23/05_SD_10.23. Authors are also thankful to sophisticated analytical instrument facilities at SAIF, IIT Bombay and Sophisticated Instrumentation Centre for Applied Research & Testing (SICART), Anand, Gujarat for providing the sophisticated analytical instrumental facilities of FEG-SEM and HRTEM.

References

1. Bao Z, Weatherspoon MR, Shian S, et al (2007) Chemical reduction of three-dimensional silica micro-assemblies into microporous silicon replicas. Nature 446:172–175. https://doi.org/10.1038/nature05570
2. Betty C (2008) Porous Silicon: A Resourceful Material for Nanotechnology. NANOTEC 2:128–136. https://doi.org/10.2174/187221008784534514

3. Boddolla S A review on Characterization techniques of Nanomaterials. International Journal of Engineering
4. Bristogianni T, Oikonomopoulou F (2022) Glass up-casting: a review on the current challenges in glass recycling and a novel approach for recycling “as-is” glass waste into volumetric glass components. Glass Struct Eng. https://doi.org/10.1007/s40940-022-00206-9
5. Chan CK, Peng H, Liu G, et al (2008) High-performance lithium battery anodes using silicon nanowires. Nat Nanotechnol 3:31–35. https://doi.org/10.1038/nnano.2007.411
6. Chandra Muduli R, Kale P (2023) Silicon nanostructures for solid-state hydrogen storage: A review. International Journal of Hydrogen Energy 48:1401–1439. https://doi.org/10.1016/j.ijhydene.2022.10.055
7. Choi M, Kim J-C, Kim D-W (2018) Waste Windshield-Derived Silicon/Carbon Nanocomposites as High-Performance Lithium-Ion Battery Anodes. Sci Rep 8:960. https://doi.org/10.1038/s41598-018-19529-1
8. Entwistle J, Rennie A, Patwardhan S (2018) A review of magnesiothermic reduction of silica to porous silicon for lithium-ion battery applications and beyond. J Mater Chem A 6:18344–18356. https://doi.org/10.1039/C8TA06370B
9. Falk G, Shinhe GP, Teixeira LB, et al (2019) Synthesis of silica nanoparticles from sugarcane bagasse ash and nano-silicon via magnesiothermic reactions. Ceramics International 45:21618–21624. https://doi.org/10.1016/j.ceramint.2019.07.157
10. Favors Z, Wang W, Bay HH, et al (2015) Scalable Synthesis of Nano-Silicon from Beach Sand for Long Cycle Life Li-ion Batteries. Sci Rep 4:5623. https://doi.org/10.1038/srep05623
11. Furquan M, Raj Khatribail A, Vijayalakshmi S, Mitra S (2018) Efficient conversion of sand to nano-silicon and its energetic Si-C composite anode design for high volumetric capacity lithium-ion battery. Journal of Power Sources 382:56–68. https://doi.org/10.1016/j.jpowsour.2018.02.011
12. Ghosh M, Khuntia S, Dalai S (2022) Effect of Molar Ratio of Feed on the Facile Synthesis of Silicon Nanosheets from Laboratory Waste Glass. In: Mukherjee K, Layek RK, De D (eds) Tailored Functional Materials. Springer Nature, Singapore, pp 131–140
13. He Y, Fan C, Lee S-T (2010) Silicon nanostructures for bioapplications. Nano Today 5:282–295. https://doi.org/10.1016/j.nantod.2010.06.008
14. Kang W, Kim J-C, Kim D-W (2020) Waste glass microfiber filter-derived fabrication of fibrous yolk-shell structured silicon/carbon composite freestanding electrodes for lithium-ion battery anodes. Journal of Power Sources 468:228407. https://doi.org/10.1016/j.jpowsour.2020.228407
15. Kang W, Kim J-C, Noh JH, Kim D-W (2019) Waste Liquid-Crystal Display Glass-Directed Fabrication of Silicon Particles for Lithium-Ion Battery Anodes. ACS Sustainable Chem Eng 7:15329–15338. https://doi.org/10.1021/acssuschemeng.9b02654
16. Kuang L, Mitchell BS, Fink MJ (2015) Silicon nanoparticles synthesised through reactive high-energy ball milling: enhancement of optical properties from the removal of iron impurities. Journal of Experimental Nanoscience 10:1214–1222. https://doi.org/10.1080/17458080.2014.989552
17. Kumar SM, Murugan K, Chandrasekhar SB, et al (2012) Synthesis and characterization of nano silicon and titanium nitride powders using atmospheric microwave plasma technique. J Chem Sci 124:557–563. https://doi.org/10.1007/s12039-012-0256-y
18. Pakuła D, Marciniec B, Przekop RE (2023) Direct Synthesis of Silicon Compounds—From the Beginning to Green Chemistry Revolution. AppliedChem 3:89–109. https://doi.org/10.3390/appliedchem3010007
19. Peng F, Wang J, Ge G, et al (2013) Photochemical reduction of CO2 catalyzed by silicon nanocrystals produced by high energy ball milling. Materials Letters 92:65–67.

https://doi.org/10.1016/j.matlet.2012.10.059
20. perrone donnorso M, Miele E, De angelis F, et al (2012) Nanoporous silicon nanoparticles for drug delivery applications. Microelectronic Engineering 98:626–629. https://doi.org/10.1016/j.mee.2012.07.095
21. Priolo F, Gregorkiewicz T, Galli M, Krauss TF (2014) Silicon nanostructures for photonics and photovoltaics. Nature Nanotech 9:19–32. https://doi.org/10.1038/nnano.2013.271
22. Rao CNR, Biswas K (2009) Characterization of Nanomaterials by Physical Methods. Annual Rev Anal Chem 2:435–462. https://doi.org/10.1146/annurev-anchem-060908-155236
23. Ryu J, Hong D, Choi S, Park S (2016) Synthesis of Ultrathin Si Nanosheets from Natural Clays for Lithium-Ion Battery Anodes. ACS Nano 10:2843–2851. https://doi.org/10.1021/acsnano.5b07977
24. Sharma R, Bisen DP, Shukla U, Sharma BG (2012) X-ray diffraction: a powerful method of characterizing nanomaterials. Recent Research in Science and Technology
25. Silviana S, Bayu WJ (2018) Silicon Conversion From Bamboo Leaf Silica By Magnesiothermic Reduction for Development of Li-ion Baterry Anode. MATEC Web Conf 156:05021. https://doi.org/10.1051/matecconf/201815605021
26. Wang H, He Y (2017) Recent Advances in Silicon Nanomaterial-Based Fluorescent Sensors. Sensors 17:268. https://doi.org/10.3390/s17020268